7536–7546 Nucleic Acids Research, 2013, Vol. 41, No. 15 Published online 14 June 2013
doi:10.1093/nar/gkt521

Conserved arginines on the rim of Hfq catalyze base pair formation and exchange

Subrata Panja[1], Daniel J. Schu[2] and Sarah A. Woodson[1,*]

[1]T.C. Jenkins Department of Biophysics, Johns Hopkins University, 3400 N. Charles Street, Baltimore, MD 21218, USA and [2]Laboratory of Molecular Biology, National Cancer Institute, Bethesda, MD 20892-5430, USA

Received March 20, 2013; Revised and Accepted May 16, 2013

ABSTRACT

The Sm-like protein Hfq is required for gene regulation by small RNAs (sRNAs) in bacteria and facilitates base pairing between sRNAs and their mRNA targets. The proximal and distal faces of the Hfq hexamer specifically bind sRNA and mRNA targets, but they do not explain how Hfq accelerates the formation and exchange of RNA base pairs. Here, we show that conserved arginines on the outer rim of the hexamer that are known to interact with sRNA bodies are required for Hfq's chaperone activity. Mutations in the arginine patch lower the ability of Hfq to act in sRNA regulation of *rpoS* translation and eliminate annealing of natural sRNAs or unstructured oligonucleotides, without preventing binding to either the proximal or distal face. Stopped-flow FRET and fluorescence anisotropy show that complementary RNAs transiently form a ternary complex with Hfq, but the RNAs are not released as a double helix in the absence of rim arginines. RNAs bound to either face of Hfq quench the fluorescence of a tryptophan adjacent to the arginine patch, demonstrating that the rim can simultaneously engage two RNA strands. We propose that the arginine patch overcomes entropic and electrostatic barriers to helix nucleation and constitutes the active site for Hfq's chaperone function.

INTRODUCTION

The Sm-like protein Hfq is an essential co-factor for post-transcriptional gene regulation by small non-coding RNA (sRNA) in bacteria [reviewed in (1)]. Many bacterial sRNAs base pair with sequences in the 5′ untranslated region of the target mRNA, stimulating or repressing translation initiation [reviewed in (2,3)], or increasing the rate of mRNA decay by RNase E [reviewed in (4–6)]. Hfq facilitates interactions between sRNAs and their mRNAs targets, increasing the rate of RNA base pairing and stabilizing the sRNA–mRNA complex (7–10). Despite abundant evidence that Hfq can promote the formation and exchange of base pairs *in vitro* (11–13), how Hfq accomplishes this remains unknown. Here, we show that conserved basic residues on the rim of Hfq are essential to its annealing and strand exchange activity, but dispensable for sequence-specific binding. We propose these residues form the active site for base pair exchange, enabling Hfq to increase the rate of sRNA–mRNA base pairing.

Bacterial Hfq is a homohexamer (67 kDa) that forms a symmetric ring and belongs to Sm/Lsm superfamily of RNA-binding proteins (7). The Sm core of Hfq is conserved (14,15) and forms two RNA-binding surfaces for single-stranded U/A-rich RNAs (16). The inner surface of the 'proximal' face of *Escherichia coli* Hfq preferentially binds U-rich RNA (15), forming a particularly stable complex with U's found at the 3′ends of sRNAs (17). The distal face binds an A-rich AAN motif (16,18) found in mRNA targets of sRNA regulation (19). A disordered 30 amino acid C-terminal extension of *E. coli* Hfq, of which the function is not understood, extends outward from the Sm core in solution (20).

Although Hfq binds its preferred substrates tightly ($\leq$20 nM); see (16,21,22), it cycles rapidly between different RNAs (23) and may diffuse along a single RNA (13). Competitive binding and *in vitro* FRET experiments showed that Hfq transiently forms a ternary complex with two complementary RNA strands before releasing the duplex and cycling off its RNA substrate (10,11,23,24). This dynamic behavior is crucial to Hfq's chaperone activity (11,12,23,25).

Translation of *E. coli rpoS* mRNA is upregulated by three different sRNAs (DsrA, RprA and ArcZ) that base pair with the *rpoS* leader and open an inhibitory stem–loop, which inhibits ribosomes binding in the absence of sRNAs (26–28). Although AAN motifs in the *rpoS* mRNA recruit the distal face of Hfq and increase the rate of sRNA annealing (19,29,30), Hfq can promote

*To whom correspondence should be addressed. Tel: +1 410 516 2015; Fax: +1 410 516 4118; Email: swoodson@jhu.edu

© The Author(s) 2013. Published by Oxford University Press.
This is an Open Access article distributed under the terms of the Creative Commons Attribution Non-Commercial License (http://creativecommons.org/licenses/by-nc/3.0/), which permits non-commercial re-use, distribution, and reproduction in any medium, provided the original work is properly cited. For commercial re-use, please contact journals.permissions@oup.com

base pairing between short RNAs lacking an U-rich or A-rich Hfq-binding site *in vitro* (30). These observations indicated that Hfq's chaperone activity is distinct from its recognition of specific RNA sequences and likely involves a separate interaction surface.

Previous work suggests that the rim or lateral edge of Hfq provides this third interaction surface. Sauer *et al*. (31) reported that sRNA bodies interact with the rim of the Sm core, and that mutations in rim arginines diminish this effect. The outer surface of the proximal face was earlier proposed to interact with tRNAs (32), and mutations at R16 in the rim diminished binding of sRNAs and double-stranded DNA (33). Rim mutations reduce binding of certain sRNA to Hfq *in vivo* and were recently found to impair positive sRNA regulation of *rpoS* and *fhlD* expression and some negative regulatory interactions (34). Thus, these studies indicated that basic residues on the rim of Hfq contribute to its biological function.

Here, we report that conserved arginines along the rim of *E. coli* Hfq are required for its RNA chaperone activity but are not required for recognition of A-rich and U-rich sequence motifs found in many mRNAs and sRNAs, respectively. Consistent with and extending previous observations that single mutations reduce Hfq's ability to act in positive regulation (34), replacement of all three arginines on the rim of Hfq with alanine greatly diminish its ability to support regulation of an *rpoS-lacZ* reporter by sRNAs. Hfq variants with rim mutations fail to facilitate sRNA binding and RNA helix formation in native polyacrylamide gel electrophoresis (PAGE) and fluorescence assays *in vitro*. Moreover, FRET and anisotropy experiments demonstrate that rim mutations slow down the dynamics of RNA binding and release, resulting in Hfq–RNA complexes that are stable but inert. Our results suggest how the arginine patch on the rim of Hfq combines with specific RNA-binding sites on the proximal and distal faces to produce a highly effective RNA chaperone.

MATERIALS AND METHODS

Hfq sequence alignment

Bacterial Hfq sequences were retrieved from UniProt, and 384 reviewed protein sequences aligned using Clustal Omega (35). This alignment was similar to that obtained for 26 different bacterial species (14) using the Cobalt Constraint-based Multiple Alignment Tool (http://www.ncbi.nlm.nih.gov/tools/cobalt/).

Bacterial strains and β-galactosidase assays

The desired *hfq* alleles were transduced into *E. coli* strains containing the *rpoS::lacZ* reporter as previously described (36) and transformed with plasmids expressing sRNAs (DsrA/RprA/ArcZ) from the *lac* promoter (pLac). Strains were WT hfq^+, PM1409 (lacI'::pBAD-rpoS576-lacZ), hfq^-, PM1419 (lacI':: pBAD-rpoS576-lacZ; Hfq::Cat), Hfq:R16A, S630207, Hfq:R16A, R17A, R19D and DJ52807. Transformants were grown in LB with arabinose (0.2%), ampicillin (100 μg/ml) and IPTG (100 μM). After growth for 4, 6 h or over-night, the OD_{600} was determined, 0.1 ml of aliquots of culture was lysed, and β-galactosidase activity was measured as described previously (8). The specific activities were calculated by $Vmax/OD_{600}$ and were the average of three independent measurements.

Hfq purification

Wild-type Hfq was overexpressed and purified using a Hi-Trap Co^{2+} column as previously described (8). The protein was free of RNA, based on absorption at 260 and 280 nm. Hfq mutants [R16A; R19A; R16K; R16A,R17A,R19D (TM); S38W; R16A,S65C] were obtained by QuikChange (Stratagene) and purified using the same protocol. R16A,S65C was treated with Cy3 maleimide (GE Healthcare) according to the manufacturer's protocol and re-purified by Hi-Trap Co^{2+} chromatography. Labeling efficiency was ~21% based on absorption at 280 and 550 nm (12).

Molecular beacon and RNA substrates

RNA molecular beacons (Supplementary Table S1) were synthesized and purified by reverse phase high-performance liquid chromatography (Trilink Biotechnologies) as previously described (12,30). Substrate oligonucleotides (Supplementary Table S1) were synthesized by Invitrogen and purified by 8% PAGE (30). Concentrations were determined by absorption at 260 nm using the manufacturer's extinction coefficient. DsrA, RprA, ArcZ56 and rpoS323 RNAs were transcribed *in vitro* as previously described (8,19).

Native gel mobility shift of sRNA and *rpoS* RNA

Hfq binding with *rpoS* mRNA (rpoS323) or sRNAs DsrA, RprA, ArcZ (56 nt) was measured at 30°C by native gel mobility shift (19). The fraction of bound RNA was fit to a single-site-binding isotherm, which approximates association of the first Hfq hexamer with the RNA. The association kinetics of ^{32}P-labeled *rpoS* mRNA leader (rpoS323) with 200 nM sRNA was measured by native gel shift (19), with or without 1 μM Hfq monomer. The fraction of counts in each lane corresponding to rpoS•DsrA (R•D) or rpoS•Hfq•DsrA (R•H•D) versus time was fit to a biphasic rate equation as described later in the text.

Fluorescent-binding assays

Changes in tryptophan fluorescence intensity were measured by exciting Hfq:S38W (1 μM) at 290 nm and recording emission at 340 nm after the addition of RNA (Fluorolog-3, Horiba). The percent quenching was calculated from $\{[I(0) - I(RNA)]/I(0)\} \times 100\%$, in which I(0) is the tryptophan emission in the absence of RNA and I(RNA) the emission in the presence of RNA. Binding assays based on the fluorescence anisotropy of D16-FAM or A18-FAM were performed as previously described (12,37).

Molecular beacon annealing assays

The association kinetics between the molecular beacon (50 nM) and the target RNA (50 nM) in TNK buffer (10 mM Tris–HCl, pH 7.5, 50 mM NaCl and 50 mM

KCl) at 30°C was measured by stopped-flow fluorescence as previously described (12). The strand exchange kinetics was measured by pre-equilibrating 50 nM rMBD16 and 50 nM D16 at 30°C for 1 h and then mixing with 50 nM cD16 in the absence or presence of Hfq (12). The normalized change in fluorescence intensity, ΔF(t), was fit to a double exponential rate equation,

$$\Delta F(t) = \frac{F(t) - F_0}{F_\infty - F_0} = A_{\text{fast}}[1 - \exp(-k_{\text{fast}}t)] + A_{\text{slow}}[1 - \exp(-k_{\text{slow}}t)]$$

in which A_{fast} and A_{slow} represent the amplitudes and k_{fast} and k_{slow} the rate constants of the fast and slow phases. The observed rate constants for five or more trials were averaged.

Hfq-binding kinetics

Association of D16-FAM (50 nM) and 500 nM Hfq-Cy3 in TNK at 30°C was measured by stopped-flow FRET as previously described (24). The decrease in the donor signal was detected using a 515-nm cut-off filter and fitted to a single or double exponential rate equation. The steady-state fluorescence polarization of D16-FAM after binding and release from Hfq was measured as described previously (24).

RESULTS

Conserved basic residues on the Hfq rim are required for sRNA regulation

Arginines at positions 16, 17 and 19 of *E. coli* Hfq form a patch of positive charge on the outer rim of the Sm core, at the top of a shallow groove leading out from the RNA-binding site along the inner surface of the proximal face (Figure 1a) (14). Alignment of 384 Hfq sequences (Supplementary Figure S1) showed that R16 is nearly invariant within this sequence collection, whereas position 17 is usually R or K (Figure 1a). Position 19 is least conserved, but frequently R, K or N. The acidic E18 side chain, which is also moderately conserved, points away from the basic patch toward the distal face.

Previous studies showed that R16 and R17 contribute to positive regulation of mRNA translation by sRNAs in *E. coli* (34), and that these effects cannot be wholly explained by poor binding and stabilization of sRNAs. To further determine whether this 'arginine patch' on the rim of the Hfq hexamer is needed for its function, we simultaneously replaced all three rim arginines with alanine or aspartate (R16A, R17A and R19D) and measured the ability of this triple mutant (TM) *hfq* allele to support up-regulation of a translational *rpoS::lacZ* fusion in *E. coli* (Figure 1b) as previously described (8). As expected, overexpression of DsrA, RprA or ArcZ sRNA from IPTG-inducible plasmids activated the expression of β-galactosidase from the *rpoS::lacZ* fusion in the presence of wild-type Hfq (Figure 1c) compared with background from endogenous DsrA in vector controls (pLac). RprA and ArcZ sRNAs were unable to increase *rpoS* expression in an *hfq* null strain, also as expected. By contrast,

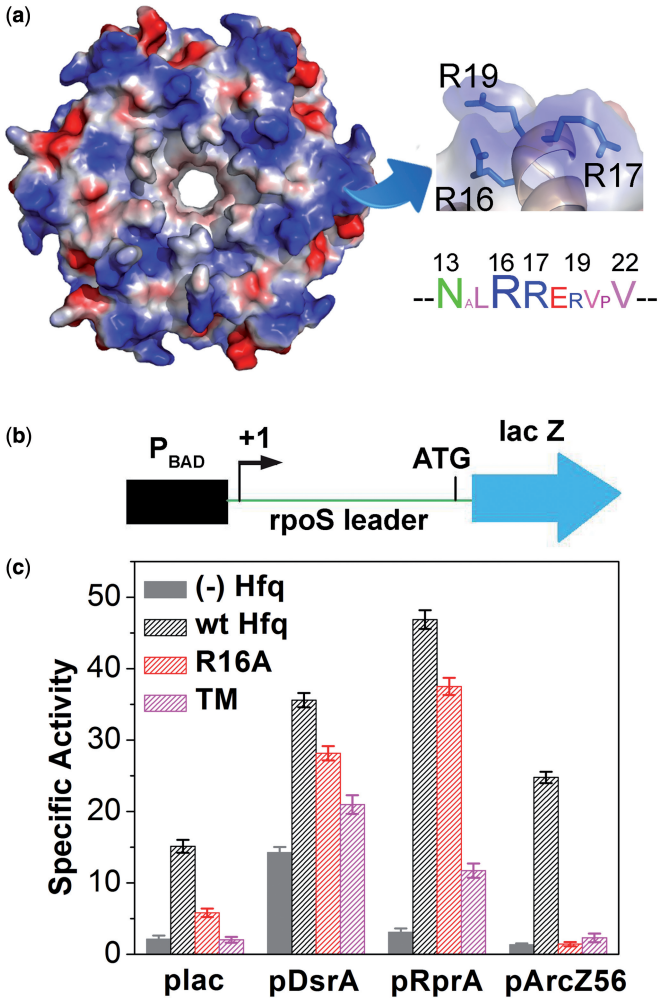

Figure 1. Conserved arginine patch on the rim of Hfq. (**a**) Electrostatic contact potentials were calculated on the surface of Hfq (*1HK9*) using PyMOL and viewed from the proximal side. Conserved arginines on the rim of Hfq (Supplementary Figure S1) are shown in detail. The disordered C-terminal 30 residues are not visible but extend from a point near the distal side of this basic patch. (**b**) *lacZ* reporter for regulation of *rpoS* translation by sRNAs was introduced into the *E. coli* chromosome under control of P_{BAD} promoter. (**c**) β-galactosidase activity in strains containing sRNA expression plasmids or pLac vector, in the presence of endogenous (WT) Hfq, or Hfq containing rim mutations.

overexpressed DsrA can partially induce *rpoS* expression in the absence of Hfq (8).

Importantly, mutation of R16 alone or of all three arginines (TM) greatly reduced the ability of sRNAs to upregulate *rpoS-lacZ* translation (Figure 1c). In the strain containing TM Hfq, ArcZ sRNA could not activate expression at all compared with the vector control. Similar results were obtained when *lac* expression was measured on MacConkey-lactose indicator plates, using a strain overexpressing ArcZ (Supplementary Figure S2). Although a R19D mutation had only a small effect in this assay, neither the R16A nor the triple *hfq* mutations supported *rpoS::lacZ* induction by ArcZ. The TM Hfq similarly impaired the ability of RprA and DsrA sRNAs to regulate *rpoS*, although these sRNAs were less strongly affected by the single R16A mutation (Figure 1c).

Together, these results showed that the rim arginines are needed for positive regulation of *rpoS* translation by sRNAs in *E. coli*.

Rim mutations do not prevent RNA binding

The mutation R16A was reported to weaken binding of sRNAs and double-stranded DNA (21). Therefore, we tested whether the arginine patch is needed for RNA binding, and if loss of binding could explain the reduced function of rim mutants *in vivo*. Semi-native gels confirmed that Hfq:R16A and other Hfq mutants formed stable hexamers (Supplementary Figure S3), although the rim mutations reduce formation of dodecamers at high-protein concentration (38,39).

Native gel mobility shift experiments (Supplementary Figure S4) showed that the R16A rim mutation had little effect on binding of Hfq to a fragment of the *rpoS* mRNA leader (rpoS323; Table 1), which interacts with the distal face of Hfq through an $(AAN)_4$ and A_6 motif (19,40) (Figure 2a). Binding of DsrA and RprA sRNA was weakened about three times (Table 1), whereas the largest change was a four-fold increase in the dissociation constant for ArcZ56 (Table 1), consistent with reduced co-immunoprecipitation of DsrA and ArcZ by Hfq:R16A (34). We used the processed 56 nt form of ArcZ sRNA for these experiments because full-length ArcZ does not anneal with *rpoS* mRNA *in vitro* (8). The triple mutant bound DsrA about as tightly as the R16A single mutant (Table 1). From these and further results described later in the text, we concluded that the rim arginines contribute to sRNA interactions but are not required for stable binding of sRNAs or mRNAs.

Rim mutants lack RNA annealing activity

Although rim mutations did not prevent Hfq from binding its substrates, loss of the arginine patch eliminated the ability of Hfq to facilitate sRNA–mRNA base pairing *in vitro*. We measured the rate of sRNA–mRNA annealing by mixing ^{32}P-labeled rpoS323 with 200 nM sRNA (DsrA, RprA or ArcZ56) and 1 μM Hfq. At various times after mixing, binary and ternary complexes were resolved by native PAGE (Supplementary Figure S5). Wild-type Hfq accelerates base pairing between DsrA and rpoS323 mRNA ~80 times (k_{obs} = 4.0 min^{-1}) compared with the same reaction in the absence of Hfq (k_{obs} = 0.05 min^{-1}; Figure 2). In the presence of the R16A and R19A single mutants, or the triple mutant (TM) Hfq, however, the annealing rate was virtually the same as in the no Hfq control (k_{obs} = 0.08 and 0.05 min^{-1}).

The Hfq rim mutants were similarly unable to facilitate annealing of RprA and ArcZ sRNAs with rpoS323 (Figure 2). This loss of activity was not because of poor RNA binding because control lanes with *rpoS* mRNA and Hfq contain the expected *rpoS*–Hfq complex (R•H; Supplementary Figure S5). It was also not explained by weakened sRNA binding because even the triple mutant retains an ability to bind DsrA (Table 1), and all three sRNAs were equally inert *in vitro*, although the R16A mutation affected their Hfq affinity to different degrees. Thus, these results suggested that the arginine patch facilitates annealing, beyond its contributions to RNA binding.

Conserved basic residues at the Hfq rim interact with RNA non-specifically

As the positively charged surface created by R16, R17 and R19 lies between the RNA-binding sites on the proximal and distal faces of the Sm core, this arginine patch could potentially interact with RNAs bound on either side of the hexamer core. To test whether RNAs interact directly with the rim of Hfq, we introduced a unique tryptophan at S38,

Table 1. Equilibrium binding constant for RNA and Hfq[a]

RNA	K_{H1} (nM)		
	WT	R16A	TM
A18	13.2	2.3	16.8
D16	22.5	39.8	17.5
CU	0.1	0.07	
DsrA	132	373	300
RprA	187	623	
ArcZ56	49	190	
rpoS323	144	196	

[a]Dissociation constants for Hfq hexamer were measured by fluorescence anisotropy (rA18, D16 and CU) or native gel mobility shift (sRNAs and rpoS323) at 30°C in TNK buffer. See Supplementary Figures S4 and S6 for details.

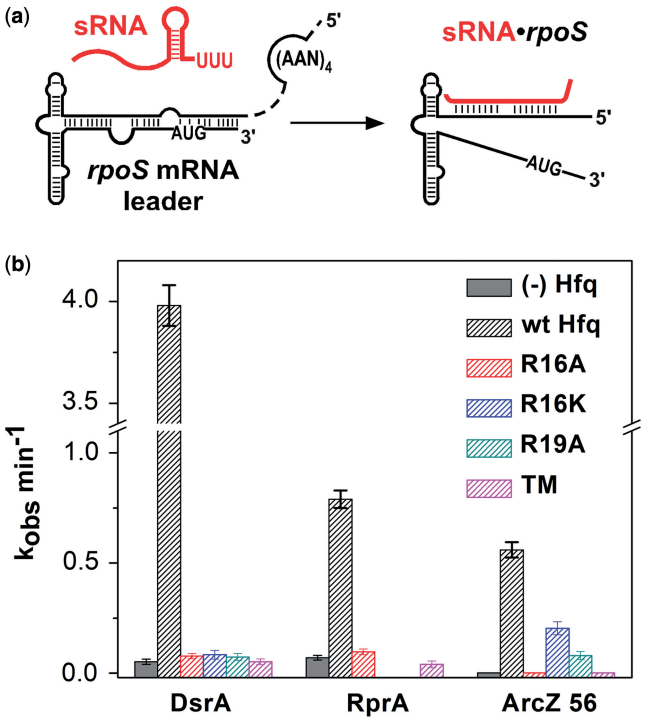

Figure 2. Rim mutants cannot facilitate annealing between sRNA and mRNA. (**a**) Annealing of ^{32}P-labeled rpoS323, 200 nM sRNA and 1 mM Hfq was measured by native gel mobility shifts (Supplementary Figure S5). (**b**) Observed rate constants for formation of the rpoS•sRNA•Hfq ternary complex for Hfq rim mutants. Gray, no Hfq; black striping, WT Hfq; red, R16A; blue, R16K; dark cyan, R19A; magenta, R16A:R17A:R19D (TM).

which lies in the shallow groove on the proximal side near R16 and should be quenched if RNA binds along the rim (Figure 3a). The fluorescence intensity of 1 μM Hfq:S38W (~170 nM hexamer) was measured after addition of different concentrations of RNAs containing either U or A-rich sequences (Figure 3b).

DsrA sRNA quenched the fluorescence of W38, indicating it interacts with the groove along the rim of the hexamer (Figure 3c) as expected (31,41). This interaction did not depend on the secondary structure of DsrA, as an unstructured 16mer containing only the internal U-rich sequence from DsrA (D16) also quenched W38 to a similar degree (Figure 3c). To further dissect the function of the arginine patch, we used a synthetic GC-rich 16-nt target sequence, which on its own binds Hfq weakly (30). This GC-rich sequence was also able to quench W38 when it was recruited to the proximal or distal face of Hfq through a U_6 or A_{18} 3′-tail, respectively (CU and CA; Figure 3c). By contrast, rU_6 (black) and rA_{18}, which bind Hfq tightly (K_d = 0.1 and 13 nM Hfq_6; Table 1) but are too short to reach the rim (15,17,18), did not quench W38 fluorescence (magenta; Figure 3c). Using fluorescence anisotropy to measure the overall affinity of these oligonucleotides (Supplementary Figure S6), we found that the R16A and TM mutations changed the apparent K_d's no more than 2-fold (Table 1).

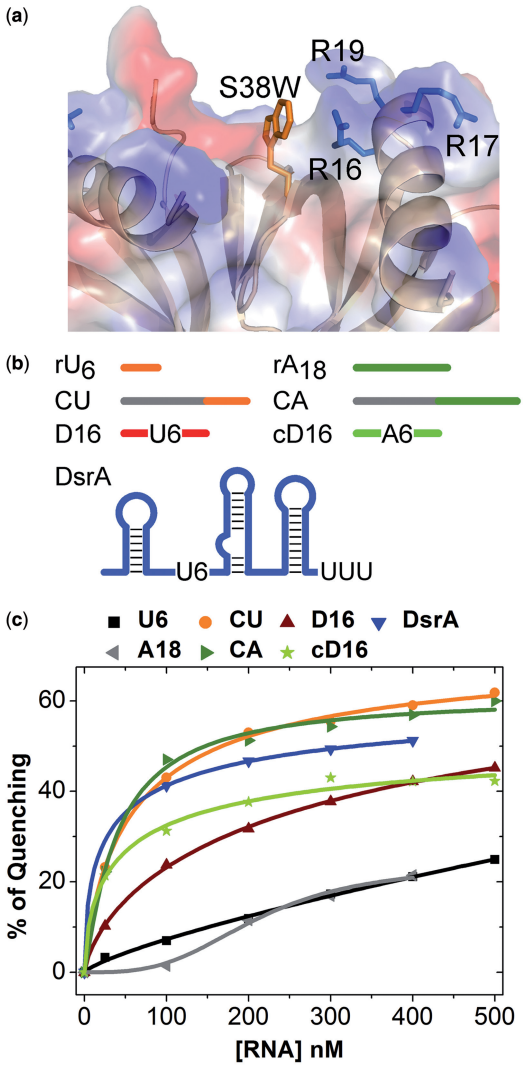

Figure 3. RNAs interact with the outer rim of Hfq. (**a**) Model of tryptophan substitution at S38 to monitor RNA binding on the rim of Hfq. (**b**) RNAs used in trp quenching experiments. DsrA and U_6 sequences (orange or red) interact with the proximal face, whereas A_{18} (dark green) binds the distal face. (**c**) Relative quenching of trp fluorescence emission (340 nm) versus RNA concentration.

From these results, we concluded that natural or synthetic RNA sequences can engage the arginine patch on the rim of Hfq, but these residues are not required for recruitment of U-rich or A-rich RNAs to the protein. We additionally inferred that the rim-binding site must have low-RNA sequence specificity, as our engineered CG-rich target sequence was able to quench W38 as potently as DsrA (compare DsrA and CU; Figure 3c). Rim interactions are also weaker than sequence-specific contacts with the proximal and distal faces, as the dissociation constant of the CG-rich sequence alone is ~1 μM compared with nanomolar dissociation constants for oligomers with an additional U_6 or A_{18} tail (30). As the degree of quenching was the same whether the RNA was anchored to Hfq by U_6 or by A_{18} (compare CU and CA), we concluded that RNAs bound to either face of Hfq interact with the arginine patch on the rim.

Rim mutation impairs annealing of short RNAs

We next used engineered oligonucleotides to dissect how the arginine patch functions in sRNA–mRNA annealing. The annealing rates were measured by stopped-flow spectroscopy, using an RNA molecular beacon that becomes more fluorescent when based paired with the target RNA (Figure 4a). When the target RNA had a 3′ A_{18} tail that binds the distal face (CA), WT Hfq accelerated annealing up to 30 times (black; Figure 4b). However, Hfq:R16A increased the rate of base pairing no more than six times above the no Hfq background (red; Figure 4b). A similar difference was observed when the target had a U_6 tail (CU; Figure 4c and d), although the annealing rate was lower for both proteins because the U_6 tail prevents release of the target from the proximal face of Hfq (30). The sensitivity of these U6 and A18 substrates to proximal and distal face mutations confirmed they bind opposite surfaces of Hfq as expected (30).

The R19A mutation, which lies toward the distal side of the hexamer, also compromised Hfq's annealing activity, but the preference for U- or A-rich substrates was opposite that of Hfq:R16A. When the target ended with A_{18}, Hfq:R19A was less active than Hfq:R16A (Figure 4b). The R19A mutant was more active than Hfq:R16A, however, when the target ended in U_6 (Figure 4d). These data suggested that the relative importance of individual side chains within the arginine patch depends on whether the RNA approaches the rim from the proximal side, nearest R16, or from the distal side, where it would first encounter R19.

The triple mutant lacking all rim arginines was completely inactive on either substrate (pink; Figure 4b and d). The triple mutant actually inhibited annealing of the

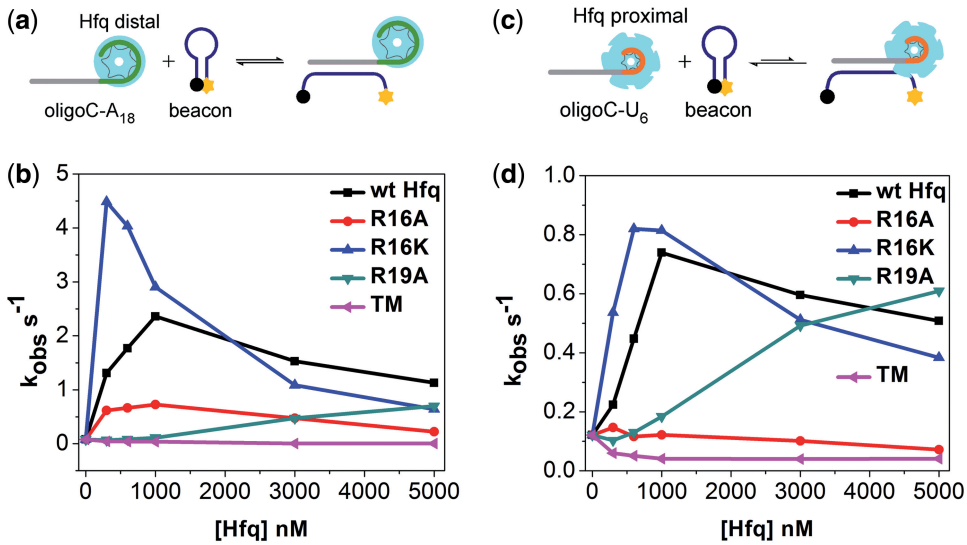

Figure 4. Basic rim patch is required for annealing U-rich and A-rich substrates. (**a**) RNA oligonucleotides for Hfq annealing assays. Base pairing of a molecular beacon (blue) with oligo CA increases FAM fluorescence. Oligo CA contains a non-specific target region (gray) and 3′ A_{18} Hfq-binding site (green). (**b**) Annealing rates were measured by stopped-flow fluorescence in TNK buffer at 30°C, using 50 nM beacon (rMBDss), 50 nM target RNA and 0–5000 nM Hfq monomer. Observed rate constants (average of five trials) are plotted against Hfq concentration. (**c**) Oligo CU contains the non-specific target region and a 3′ U_6 Hfq-binding site (orange). (**d**) Observed annealing rates for oligo CU as in (b).

CU oligomer compared with the no Hfq control, presumably because this protein forms a stable yet inactive complex with the U-rich substrate. Thus, although the rim arginines play slightly different roles in engaging RNAs from the proximal or distal faces of the hexamer, removal of all three rim arginines results in total loss of annealing activity, even toward unstructured RNAs that bind mutated Hfq with high affinity.

Lysine cannot replace R16 for Hfq function on long RNAs

As residue 16 is nearly always arginine in bacterial Hfq's, we asked whether the positive charge alone is important for its chaperone function. When R16 was replaced with lysine, Hfq:R16K also increased the initial rate of base pairing between unstructured CA and CU RNAs and an RNA molecular beacon (blue; Figure 4b and d) but was only partially able to facilitate base pairing between sRNAs and rpoS323 (Supplementary Figure S5). Although a small fraction of ^{32}P-labeled *rpoS* mRNA immediately shifted into a ternary complex with DsrA and Hfq:R16K, the remaining ternary complex formed slowly. As base pairing between DsrA and *rpoS* mRNA is needed for a ternary complex stable enough to be trapped in the native gel (40), this result suggested that some base pairing occurs rapidly, but other Hfq:R16K complexes do not progress toward a base paired state. With ArcZ56, Hfq:R16K ternary complexes appeared at rates intermediate between those of WT and R16A Hfq (Supplementary Figure S5).

These results suggested that the positive charge of the arginine patch is important for annealing activity, but R16 may contribute to recognition or restructuring of long RNAs. This idea was supported by the reduced activity of the R16K mutant in a strand exchange assay (Supplementary Figure S7), which requires interaction with a double-stranded substrate. Although WT Hfq increased the rate of strand exchange 90 times compared with no Hfq, Hfq:R16A was unable to do so at all, whereas Hfq:R16K and Hfq:R19A increased the rate only 10 times (Supplementary Figure S7c). Thus, the arginines on both sides of the rim of Hfq are needed for strand exchange as well as for optimal annealing.

Rim mutation impairs RNA cycling on Hfq

During the annealing cycle, Hfq rapidly binds two single-stranded RNAs in a transient ternary complex, then releases the newly formed duplex (24). In natural substrates, Hfq remains bound to A-rich motifs in the *rpoS* mRNA, resulting in stable ternary complexes that can be seen in native gels after the RNAs have base paired (40). Short RNAs lacking an A-rich-binding site for Hfq are rapidly released into solution when the complementary regions base pair (24). If the arginine patch is directly involved in the formation and exchange of RNA base pairs, at least one of these binding and release steps should be defective in the R16A mutant.

To test this, we first directly measured the RNA-binding rate by stopped-flow FRET, using FAM-labeled D16 RNA and Cy3-labeled Hfq (Figure 5a). WT Hfq binds D16 with two kinetic phases, in which the fast phase ($37\,s^{-1}$) contributes most directly to rapid annealing of short oligonucleotides (24). By contrast, we observed only the slow binding phase ($0.6\,s^{-1}$) for the R16A mutant (Figure 5b and Supplementary Figure S8a–c), implying less dynamic RNA–Hfq interactions, even though D16 RNA binds Hfq:R16A less tightly than WT Hfq overall (Table 1).

We next attempted to directly observe turnover of Hfq ternary complexes using fluorescence anisotropy, which is sensitive to the hydrodynamic size and thus molecular weight of the complex (Figure 5c). When 83 nM WT

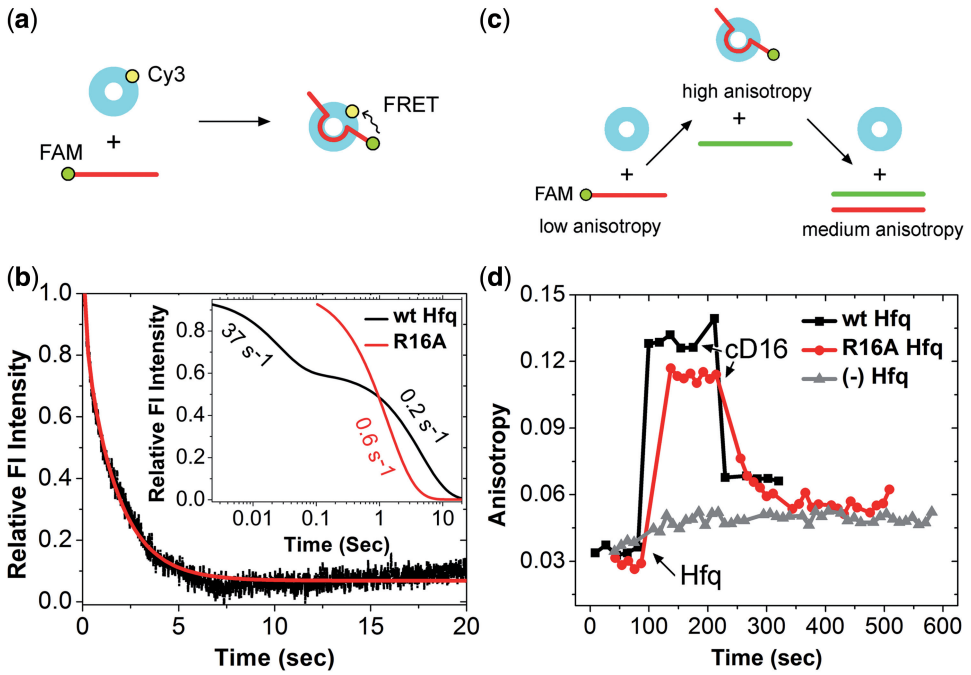

Figure 5. Rim arginines catalyze rapid single-strand binding and duplex release. (**a**) FRET assay for Hfq binding. When D16 RNA binds Cy3-labeled Hfq, energy transfer reduces the fluorescence emission of the FAM donor. (**b**) After mixing 50 nM D16-FAM RNA with 500 nM Cy3-labeled R16A Hfq, the decrease in FAM emission because of FRET was fit to a single exponential rate equation, assuming one RNA binds each hexamer. Fitted curves compare the binding kinetics of WT and R16A Hfq (inset). (**c**) Detection of ternary and binary complexes by anisotropy. (**d**) Steady-state anisotropy of 50 nM D16-FAM, after mixing with 100 nM Hfq_6 and addition of complementary RNA (50 nM cD16) a few minutes later (arrows). Black, WT Hfq; red, Hfq:R16A; gray, no Hfq. The rise in anisotropy because of Hfq-independent base pairing (gray) and the decrease in the anisotropy of the R16A ternary complex were fit to single-exponential rate equations (data not shown), yielding observed rate constants of 0.018 and 0.02 s^{-1}, respectively.

Hfq_6 was added to 50 nM D16-FAM, the anisotropy of the RNA jumped from 0.035 to 0.127 (Figure 5d), as expected given that binding is faster than the anisotropy measurement time [Supplementary Figure S8b; (24)]. When complementary cD16 RNA was added to the D16-Hfq complex, a brief spike in anisotropy (0.14) corresponding to formation of the ternary complex was followed by a rapid decrease in anisotropy to 0.074 indicating Hfq release from the D16-cD16 duplex (black; Figure 5d). The final anisotropy was only slightly higher than that of D16-cD16 alone (gray; Figure 5d), suggesting that most of the RNA was released from Hfq.

When the same experiment was done with Hfq:R16A (red; Figure 5d), the anisotropy again increased, indicating that D16-FAM was able to bind as expected. When cD16 RNA was added to the Hfq•D16 complex, however, the anisotropy dropped slowly, requiring several minutes to reach the anisotropy of the RNA duplex. Importantly, the rate constant for this change, 0.021 s^{-1}, was the same within error as the rate of base pairing in the absence of Hfq (0.018 s^{-1}, gray; Figure 5d). This can be explained by occasional dissociation of D16 RNA from Hfq and base pairing of the two RNA strands in solution. Taken together, the FRET and anisotropy results showed that the R16A mutant binds D16 RNA, but forms passive complexes that do not accelerate the formation and release of double helices, in agreement with the results of our annealing assays.

The results of the anisotropy experiment were confirmed by stopped-flow FRET assays, which showed that double-stranded RNA is rapidly released from WT but not R16A Hfq (Supplementary Figure S8d–f). Similarly, addition of D16-FAM RNA to Hfq-Cy3 in the presence of a complementary RNA strand showed that it binds and dissociates from WT Hfq in less than a second (Supplementary Figure S8h) and (24). By contrast, D16-FAM RNA failed to dissociate from Hfq:R16A within our 20 s observation window (Supplementary Figure S8i). Therefore, the R16A rim mutation eliminates the dynamic exchange of RNA strands intrinsic to Hfq's annealing activity.

DISCUSSION

An active site for RNA annealing

sRNA regulation of gene expression relies on efficient binding of sRNAs to their mRNA targets, which is facilitated by the abundant bacterial Sm-like protein Hfq. Hfq has been long known to interact with both U-rich and A-rich single strands (42,43) and seems to raise the effective stability of sRNA–mRNA complexes as well as increase the binding kinetics (7,8). More recently, Sauer *et al.* (31) proposed that interactions with the rim remodel the sRNA body and consequently enhance base pairing with another RNA. Nonetheless, these binding surfaces of the Hfq hexamer do not fully explain how Hfq accelerates base pairing of short (unstructured) RNAs lacking a U or A-rich sequence (30).

Here, we demonstrate that the highly conserved arginine patch on the rim of the Hfq hexamer constitutes an active

site for helix formation and strand exchange, accelerating base pair formation by forming dynamic and non-specific interactions with RNAs recruited to the distal and proximal faces of the hexamer (Figure 6). Release of the double-stranded product resets the arginine patch active site for another cycle of helix formation.

Rim mutations reduced or eliminated the ability of Hfq to anneal natural substrates and short oligonucleotides (Figures 3 and 4). Moreover, the R16A mutation eliminated rapid binding and release of short RNAs from the Hfq hexamer, indicating that the intrinsic dynamics of the RNA–Hfq complexes were changed. Displacement of an RNA oligonucleotide is normally efficient and rapid (20–30 s^{-1}) when a complementary strand is added to the reaction because the newly formed duplex binds Hfq much less well than the single strands (24). By contrast, Hfq:R16A failed to release bound RNA when the complementary RNA was added (Figure 5 and Supplementary Figure S8), implying that the mutant protein was unable to promote base pairing.

Several observations suggest this loss of activity is not merely the result of poor RNA binding. Not only do rim mutations inhibit sRNA annealing much more than they reduce sRNA binding, but the rim mutations do not affect recruitment of Hfq to the *rpoS* mRNA, which is critical for sRNA annealing (40) and regulation (8). The triple Hfq mutant (lacking all rim arginines) binds short RNAs with normal (WT) affinity and DsrA about three times less tightly than WT Hfq, yet has no measurable annealing activity on any substrate. We also noted that poor annealing of short RNAs was not overcome by increased Hfq concentration, as might be expected if the rim mutations weakened substrate binding but not catalysis of helix formation (Figure 4).

The rim arginines, and particularly R16, do contribute to binding of natural sRNAs in our experiments, as previously reported (31). We suggest this is because R16 specifically interacts with double-stranded regions of the sRNA, or because the arginine patch partially unwinds structured RNAs as suggested by solution scattering studies (44,45), allowing for more extensive interactions with the surface of Hfq. It could also arise from changes in the conformation of Hfq caused by the rim mutations. Regardless, Hfq's ability to accelerate the association of unstructured oligonucleotides as much as several hundred times (12,30) cannot be explained by specific binding of sRNAs as proposed by Sauer *et al.* (31). The arginine patch is essential to this intrinsic annealing activity, beyond any ability to remodel sRNAs.

The arginine patch overcomes barriers to helix nucleation

Early studies of RNA relaxation kinetics demonstrated that nucleation of the double helix is slower than diffusion (46,47), whereas the remaining base pairs 'zipper' rapidly

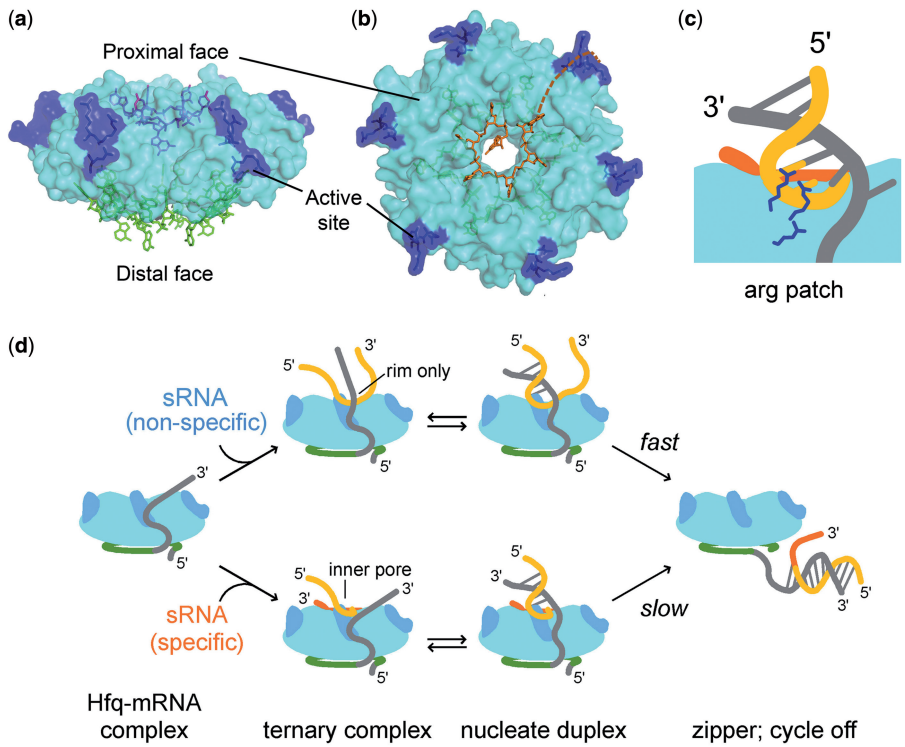

Figure 6. Model for Hfq-dependent RNA annealing. (**a**) Superposition of *E. coli* Hfq [*3GIB*; (18)] and *S. aureus* Hfq [*1KQ2*; (15)], showing A_{18} bound to the distal face (green) and 5′AU_5G bound on the proximal face (orange). Arginine patch on the rim of Hfq (blue) catalyzes base pair formation and exchange. (**b**) View of the proximal face, showing hypothetical path (orange) from inner pore to active site. (**c**) Cartoon of arginines contacting RNA in active site. (**d**) Model for annealing. The distal face of Hfq binds mRNA AAN motifs (green). Unstructured RNAs (gold) engage the proximal side of the rim non-specifically (top). The sRNA U_6 tail (orange) binds the proximal pore (bottom). After helix nucleation in the rim active site, zippering of the complementary region leads to dissociation of the double helix from the proximal face of Hfq. Release is slower when the sRNA is tightly bound to the proximal side (bottom).

(1 μs) once the first 2–3 bp of the helix have formed (48). In the absence of sufficient base stacking, helix nucleation is unfavorable owing to the loss of configurational entropy in the RNA and electrostatic repulsion of the phosphates (49). Thus, nucleation of the double helix limits the observed rate of helix formation.

Our model suggests how Hfq overcomes these barriers to helix nucleation, increasing the rate of helix formation 10–10 000-fold (24). First, co-localization of the sRNA and mRNA by recruitment of adjacent U- and A-rich sequences to the proximal and distal faces, reduces the entropic penalty for bringing two strands together (7). Second, the positive charge of the arginine patch reduces the electrostatic barrier to base pairing between complementary nucleotides, as predicted from the classical dependence of helix formation rates on ionic strength (50). Other positively charged RNA-binding proteins, such as HIV nucleocapsid (NCp7) and *E. coli* StpA, promote base pairing through electrostatic interactions with the RNA (51,52) and have a strong aggregating activity that promotes strand association. Third, as the R16K substitution also alters Hfq's activity, the arginine side chains may directly stabilize nascent Watson–Crick base pairs by forming bidentate hydrogen bonds with the minor groove face, as occurs in DNA polymerases (53). A role for R16 in dsRNA binding is suggested by weaker binding of the R16A mutant to dsDNA and a double-stranded domain of DsrA sRNA (33,37), and the proposed role of the rim in sRNA binding and exchange (31).

Mechanism of sRNA–mRNA annealing

The arginine patch on the rim of Hfq is perfectly situated to align RNA strands bound to the proximal and distal faces, and to form dynamic and flexible interactions with the sRNA seed sequence and its mRNA complement (Figure 6). Tryptophan quenching experiments (Figure 2) with oligonucleotides containing a U6 or A18 3′ tail confirm that the arginine patch is accessible from both faces of the hexamer and further indicate that interactions at the rim are weak [~1 μM monomer; (30)] with low-sequence selectivity. Therefore, we infer that sequence-specific recruitment of sRNAs and mRNAs to the proximal and distal faces, respectively, positions adjacent nucleotides from each RNA to interact with the arginine patch and with each other (Figure 6a). This combination of specific and non-specific binding sites explains how Hfq is targeted to sRNAs and mRNAs RNAs as a class, yet can anneal a wide variety of antisense sequences (16,54). Sauer *et al*. (31) found that sRNA interacts the lateral rim of Hfq, and based on this proposed that the arginine patch on the rim orients sRNAs to form new base pairing interactions.

A minimal model for each annealing cycle is illustrated in Figure 6b. We assume for simplicity that the distal face of Hfq initially binds an A-rich motif in the mRNA (green; Figure 6b), as recruitment of Hfq to the mRNA is highly important for sRNA regulation (8,19,29,55). As recruitment of the distal face to an A-rich sequence greatly increases the annealing rate, whereas recruitment of the proximal face to a U_6 sequence does not, we propose that distal face binding places the target sequence where it can engage the arginine patch. This is further supported by the deleterious effect of the R19A mutation when the target RNA is recruited to the distal face of Hfq (Figure 4b).

With mRNA bound to the distal face, the proximal side of the arginine patch is free to bind a few residues from an sRNA or other RNA segment. As short, unstructured RNAs bind and dissociate from Hfq rapidly [30–40 s^{-1}; (24)], we expect that non-specific interactions with the rim will be dynamic, allowing random sampling of nearby bases (top path; Figure 6b). If two complementary sequences engage the arginine patch, successful nucleation of the double helix leads to release of the duplex and complete zippering of the sRNA•mRNA helix (10). When U-rich sequences in the sRNA bind the inner surface of the proximal face, annealing should be more efficient (bottom path; Figure 6b). However, we expect that such sRNA–mRNA pairs will release Hfq more slowly, unless the sRNA is actively displaced by another RNA (23).

Depending on the intracellular RNA concentrations and the stability of the sRNA–mRNA base pairing, efficient annealing by Hfq can increase the effective concentration of the sRNA–mRNA duplex (8). Transfer of Hfq between binding sites within the same RNA (19) or to another RNA (23) is also expected to stabilize the sRNA–mRNA duplex, leading to an apparent effect on the annealing equilibrium.

This model raises many questions yet to be investigated. First, co-precipitation experiments show that Hfq binds directly to many sRNAs *in vivo* (56,57). We do not know whether the sRNAs bring Hfq to the mRNA, or transfer to the mRNA-bound Hfq, or if annealing can even occur between RNAs bound to two different hexamers. Second, the molecular details of RNA binding at the rim are not yet known, nor is it known how the RNAs strands move with respect to the arginine patch and whether more than one arginine patch is required for activity. Finally, the N- and C-terminal peptides, whose function remains unclear (58,59), extend from the rim near the arginine patch. These intrinsically disordered regions of Hfq (20) could conceivably assist RNA binding along the rim, or modulate the dynamics of RNA binding and release.

Implications for sRNA regulation

Nearly all bacterial Hfq proteins have arginine at position 16, making it one of the most conserved residues in the protein. Although γ-proteobacteria have an RRER rim sequence that we predict is highly active in RNA annealing, this motif can have fewer arginines, particularly in Gram-positive bacteria (14) as previously noted by Sauer *et al*. (31). Among the Gram-positive bacteria in which the function of Hfq has been characterized, there exists an anecdotal correlation between the number of arginines (or lysines) at the rim and the function of Hfq in sRNA regulation: Hfq from *Listeria monocytogenes* (RKEK) was reported to stabilize sRNA–mRNA complexes (60), but *Bacillus subtilis* Hfq (RKEN) may not be required for sRNA regulation (61,62). *Staphylococcus aureus* Hfq is

one of the rare examples with a lysine at position 16 (KANQ; Supplementary Figure S1). Its function in sRNA-dependent regulation is presently unclear (63,64) but seems to differ from that of enteric γ-proteobacteria (65). Although eukaryotic Lsm proteins lack the RRER motif, human Lsm proteins (apart from Lsm1 and Lsm8) contain at least one basic residue within this loop (66).

The degree to which the arginine patch is required to facilitate sRNA–mRNA interactions may also vary among sRNAs in *E. coli*. *In vivo* reporter assays showed that R16 and R17 were important for upregulation of *rpoS* and *flhD* by ArcZ and McaS, respectively, and negative regulation of *fhlD* by ArcZ (34). However, the same rim mutations had little effect on negative regulation of *sdhCDAB* and *sodB* by RyhB. Thus, the importance of the arginine patch to a particular regulatory interaction may reflect the degree to which an sRNA can anneal with an mRNA target without the help of Hfq, and whether Hfq must release the sRNA or recruit additional proteins such as RNase E to the sRNA–mRNA complex (67). Our finding that the arginine patch acts in RNA annealing should help dissect these regulatory mechanisms.

SUPPLEMENTARY DATA

Supplementary Data are available at NAR Online: Supplementary Table 1 and Supplementary Figures 1–8.

ACKNOWLEDGEMENTS

The authors thank X. Zheng, K. Doxzen, Y. Peng and G. Chelapa for technical help, and T. Updegrove, G. Storz, A. Zhang, N. Majdalani and S. Gottesman for discussion.

FUNDING

National Institute of General Medicine [R01 GM46686 to S.W.] and the intramural research program of the National Cancer Institute [to D.J.S.]. Funding for open access charge: National Institutes of Health.

Conflict of interest statement. None declared.

REFERENCES

1. Vogel,J. and Luisi,B.F. (2011) Hfq and its constellation of RNA. *Nat. Rev. Microbiol.*, **9**, 578–589.
2. Gottesman,S., McCullen,C.A., Guillier,M., Vanderpool,C.K., Majdalani,N., Benhammou,J., Thompson,K.M., FitzGerald,P.C., Sowa,N.A. and FitzGerald,D.J. (2006) Small RNA regulators and the bacterial response to stress. *Cold Spring Harb. Symp. Quant. Biol.*, **71**, 1–11.
3. Beisel,C.L. and Storz,G. (2010) Base pairing small RNAs and their roles in global regulatory networks. *FEMS Microbiol. Rev.*, **34**, 866–882.
4. Kaberdin,V.R. and Blasi,U. (2006) Translation initiation and the fate of bacterial mRNAs. *FEMS Microbiol. Rev.*, **30**, 967–979.
5. Caron,M.P., Lafontaine,D.A. and Masse,E. (2010) Small RNA-mediated regulation at the level of transcript stability. *RNA Biol.*, **7**, 140–144.
6. Aiba,H. (2007) Mechanism of RNA silencing by Hfq-binding small RNAs. *Curr. Opin. Microbiol.*, **10**, 134–139.
7. Zhang,A., Wassarman,K.M., Ortega,J., Steven,A.C. and Storz,G. (2002) The Sm-like Hfq Protein Increases OxyS RNA Interaction with Target mRNAs. *Mol. Cell*, **9**, 11–22.
8. Soper,T., Mandin,P., Majdalani,N., Gottesman,S. and Woodson,S.A. (2010) Positive regulation by small RNAs and the role of Hfq. *Proc. Natl Acad. Sci. USA*, **107**, 9602–9607.
9. Moller,T., Franch,T., Hojrup,P., Keene,D.R., Bachinger,H.P., Brennan,R.G. and Valentin-Hansen,P. (2002) Hfq: a bacterial Sm-like protein that mediates RNA-RNA interaction. *Mol. Cell*, **9**, 23–30.
10. Lease,R.A. and Woodson,S.A. (2004) Cycling of the Sm-like protein Hfq on the DsrA small regulatory RNA. *J. Mol. Biol.*, **344**, 1211–1223.
11. Rajkowitsch,L. and Schroeder,R. (2007) Dissecting RNA chaperone activity. *RNA*, **13**, 2053–2060.
12. Hopkins,J.F., Panja,S., McNeil,S.A. and Woodson,S.A. (2009) Effect of salt and RNA structure on annealing and strand displacement by Hfq. *Nucleic Acids Res.*, **37**, 6205–6213.
13. Arluison,V., Hohng,S., Roy,R., Pellegrini,O., Regnier,P. and Ha,T. (2007) Spectroscopic observation of RNA chaperone activities of Hfq in post-transcriptional regulation by a small non-coding RNA. *Nucleic Acids Res.*, **35**, 999–1006.
14. Sun,X., Zhulin,I. and Wartell,R.M. (2002) Predicted structure and phyletic distribution of the RNA-binding protein Hfq. *Nucleic Acids Res.*, **30**, 3662–3671.
15. Schumacher,M.A., Pearson,R.F., Moller,T., Valentin-Hansen,P. and Brennan,R.G. (2002) Structures of the pleiotropic translational regulator Hfq and an Hfq-RNA complex: a bacterial Sm-like protein. *EMBO J.*, **21**, 3546–3556.
16. Mikulecky,P.J., Kaw,M.K., Brescia,C.C., Takach,J.C., Sledjeski,D.D. and Feig,A.L. (2004) *Escherichia coli* Hfq has distinct interaction surfaces for DsrA, rpoS and poly(A) RNAs. *Nat. Struct. Mol. Biol.*, **11**, 1206–1214.
17. Sauer,E. and Weichenrieder,O. (2011) Structural basis for RNA 3′-end recognition by Hfq. *Proc. Natl Acad. Sci. USA*, **108**, 13065–13070.
18. Link,T.M., Valentin-Hansen,P. and Brennan,R.G. (2009) Structure of *Escherichia coli* Hfq bound to polyriboadenylate RNA. *Proc. Natl Acad. Sci. USA*, **106**, 19292–19297.
19. Soper,T.J. and Woodson,S.A. (2008) The rpoS mRNA leader recruits Hfq to facilitate annealing with DsrA sRNA. *RNA*, **14**, 1907–1917.
20. Beich-Frandsen,M., Vecerek,B., Konarev,P.V., Sjoblom,B., Kloiber,K., Hammerle,H., Rajkowitsch,L., Miles,A.J., Kontaxis,G., Wallace,B.A. *et al.* (2011) Structural insights into the dynamics and function of the C-terminus of the *E. coli* RNA chaperone Hfq. *Nucleic Acids Res.*, **39**, 4900–4915.
21. Updegrove,T.B. and Wartell,R.M. (2011) The influence of *Escherichia coli* Hfq mutations on RNA binding and sRNA*mRNA duplex formation in rpoS riboregulation. *Biochim. Biophys. Acta*, **1809**, 532–540.
22. Olejniczak,M. (2011) Despite similar binding to the Hfq protein regulatory RNAs widely differ in their competition performance. *Biochemistry*, **50**, 4427–4440.
23. Fender,A., Elf,J., Hampel,K., Zimmermann,B. and Wagner,E.G. (2010) RNAs actively cycle on the Sm-like protein Hfq. *Genes Dev.*, **24**, 2621–2626.
24. Hopkins,J.F., Panja,S. and Woodson,S.A. (2011) Rapid binding and release of Hfq from ternary complexes during RNA annealing. *Nucleic Acids Res.*, **39**, 5193–5202.
25. Adamson,D.N. and Lim,H.N. (2011) Essential requirements for robust signaling in Hfq dependent small RNA networks. *PLoS Comput. Biol.*, **7**, e1002138.
26. Majdalani,N., Cunning,C., Sledjeski,D., Elliott,T. and Gottesman,S. (1998) DsrA RNA regulates translation of RpoS message by an anti-antisense mechanism, independent of its action as an antisilencer of transcription. *Proc. Natl Acad. Sci. USA*, **95**, 12462–12467.
27. Majdalani,N., Chen,S., Murrow,J., St John,K. and Gottesman,S. (2001) Regulation of RpoS by a novel small RNA: the characterization of RprA. *Mol. Microbiol.*, **39**, 1382–1394.
28. Lease,R.A., Cusick,M.E. and Belfort,M. (1998) Riboregulation in *Escherichia coli*: DsrA RNA acts by RNA:RNA interactions at multiple loci. *Proc. Natl Acad. Sci. USA*, **95**, 12456–12461.

29. Updegrove,T., Wilf,N., Sun,X. and Wartell,R.M. (2008) Effect of Hfq on RprA-rpoS mRNA pairing: Hfq-RNA binding and the influence of the 5′ rpoS mRNA leader region. *Biochemistry*, **47**, 11184–11195.
30. Panja,S. and Woodson,S.A. (2012) Hfq proximity and orientation controls RNA annealing. *Nucleic Acids Res.*, **40**, 8690–8697.
31. Sauer,E., Schmidt,S. and Weichenrieder,O. (2012) Small RNA binding to the lateral surface of Hfq hexamers and structural rearrangements upon mRNA target recognition. *Proc. Natl Acad. Sci. USA*, **109**, 9396–9401.
32. Lee,T. and Feig,A.L. (2008) The RNA binding protein Hfq interacts specifically with tRNAs. *RNA*, **14**, 514–523.
33. Updegrove,T.B., Correia,J.J., Galletto,R., Bujalowski,W. and Wartell,R.M. (2010) *E. coli* DNA associated with isolated Hfq interacts with Hfq's distal surface and C-terminal domain. *Biochim. Biophys. Acta*, **1799**, 588–596.
34. Zhang,A., Schu,D.J., Tjaden,B.C., Storz,G. and Gottesman,S. (2013) Mutations in interaction surfaces differentially impact *E. coli* Hfq association with small RNAs and their mRNA targets. *J. Mol. Biol.*, in press. doi: 10.1016/j.jmb.2013.01.006.
35. Sievers,F., Wilm,A., Dineen,D., Gibson,T.J., Karplus,K., Li,W., Lopez,R., McWilliam,H., Remmert,M., Soding,J. *et al.* (2011) Fast, scalable generation of high-quality protein multiple sequence alignments using Clustal Omega. *Mol. Syst. Biol.*, **7**, 539.
36. Mandin,P. and Gottesman,S. (2010) Integrating anaerobic/aerobic sensing and the general stress response through the ArcZ small RNA. *EMBO J.*, **29**, 3094–3107.
37. Sun,X. and Wartell,R.M. (2006) *Escherichia coli* Hfq binds A18 and DsrA domain II with similar 2:1 Hfq6/RNA stoichiometry using different surface sites. *Biochemistry*, **45**, 4875–4887.
38. Panja,S. and Woodson,S.A. (2012) Hexamer to monomer equilibrium of *E. coli* Hfq in solution and its impact on RNA annealing. *J. Mol. Biol.*, **417**, 406–412.
39. Wang,W., Wang,L., Zou,Y., Zhang,J., Gong,Q., Wu,J. and Shi,Y. (2011) Cooperation of *Escherichia coli* Hfq hexamers in DsrA binding. *Genes Dev.*, **25**, 2106–2117.
40. Soper,T.J., Doxzen,K. and Woodson,S.A. (2011) Major role for mRNA binding and restructuring in sRNA recruitment by Hfq. *RNA*, **17**, 1544–1550.
41. Brescia,C.C., Mikulecky,P.J., Feig,A.L. and Sledjeski,D.D. (2003) Identification of the Hfq-binding site on DsrA RNA: Hfq binds without altering DsrA secondary structure. *RNA*, **9**, 33–43.
42. Senear,A.W. and Steitz,J.A. (1976) Site-specific interaction of Qbeta host factor and ribosomal protein S1 with Qbeta and R17 bacteriophage RNAs. *J. Biol. Chem.*, **251**, 1902–1912.
43. de Haseth,P.L. and Uhlenbeck,O.C. (1980) Interaction of *Escherichia coli* host factor protein with oligoriboadenylates. *Biochemistry*, **19**, 6138–6146.
44. Vincent,H.A., Henderson,C.A., Stone,C.M., Cary,P.D., Gowers,D.M., Sobott,F., Taylor,J.E. and Callaghan,A.J. (2012) The low-resolution solution structure of Vibrio cholerae Hfq in complex with Qrr1 sRNA. *Nucleic Acids Res.*, **40**, 8698–8710.
45. Ribeiro Ede,A. Jr, Beich-Frandsen,M., Konarev,P.V., Shang,W., Vecerek,B., Kontaxis,G., Hammerle,H., Peterlik,H., Svergun,D.I., Blasi,U. *et al.* (2012) Structural flexibility of RNA as molecular basis for Hfq chaperone function. *Nucleic Acids Res.*, **40**, 8072–8084.
46. Craig,M.E., Crothers,D.M. and Doty,P. (1971) Relaxation kinetics of dimer formation by self complementary oligonucleotides. *J. Mol. Biol.*, **62**, 383–401.
47. Porschke,D. and Eigen,M. (1971) Co-operative non-enzymic base recognition. 3. Kinetics of the helix-coil transition of the oligoribouridylic–oligoriboadenylic acid system and of oligoriboadenylic acid alone at acidic pH. *J. Mol. Biol.*, **62**, 361–381.
48. Porschke,D. (1974) A direct measurement of the unzippering rate of a nucleic acid double helix. *Biophys. Chem.*, **2**, 97–101.
49. Turner,D.H. (2000) In: Bloomfield,V.A., Tinoco,I.J. and Crothers,D.M. (eds), *Nucleic Acids: Structures, Properties, Functions*. University Science Books, Sausalito, pp. 259–334.
50. Porschke,D., Uhlenbec,O.C. and Martin,F.H. (1973) Thermodynamics and kinetics of helix-coil transition of oligomers containing GC base pairs. *Biopolymers*, **12**, 1313–1335.
51. Levin,J.G., Guo,J., Rouzina,I. and Musier-Forsyth,K. (2005) Nucleic acid chaperone activity of HIV-1 nucleocapsid protein: critical role in reverse transcription and molecular mechanism. *Prog. Nucleic Acid Res. Mol. Biol.*, **80**, 217–286.
52. Doetsch,M., Gstrein,T., Schroeder,R. and Furtig,B. (2010) Mechanisms of StpA-mediated RNA remodeling. *RNA Biol.*, **7**, 735–743.
53. Doublie,S., Tabor,S., Long,A.M., Richardson,C.C. and Ellenberger,T. (1998) Crystal structure of a bacteriophage T7 DNA replication complex at 2.2 A resolution [see comments]. *Nature*, **391**, 251–258.
54. Storz,G., Opdyke,J.A. and Zhang,A. (2004) Controlling mRNA stability and translation with small, noncoding RNAs. *Curr. Opin. Microbiol.*, **7**, 140–144.
55. Desnoyers,G. and Masse,E. (2012) Noncanonical repression of translation initiation through small RNA recruitment of the RNA chaperone Hfq. *Genes Dev.*, **26**, 726–739.
56. Zhang,A., Wassarman,K.M., Rosenow,C., Tjaden,B.C., Storz,G. and Gottesman,S. (2003) Global analysis of small RNA and mRNA targets of Hfq. *Mol. Microbiol.*, **50**, 1111–1124.
57. Sittka,A., Lucchini,S., Papenfort,K., Sharma,C.M., Rolle,K., Binnewies,T.T., Hinton,J.C. and Vogel,J. (2008) Deep sequencing analysis of small noncoding RNA and mRNA targets of the global post-transcriptional regulator, Hfq. *PLoS Genet.*, **4**, e1000163.
58. Vecerek,B., Rajkowitsch,L., Sonnleitner,E., Schroeder,R. and Blasi,U. (2008) The C-terminal domain of *Escherichia coli* Hfq is required for regulation. *Nucleic Acids Res.*, **36**, 133–143.
59. Olsen,A.S., Moller-Jensen,J., Brennan,R.G. and Valentin-Hansen,P. (2010) C-terminally truncated derivatives of *Escherichia coli* Hfq are proficient in riboregulation. *J. Mol. Biol.*, **404**, 173–182.
60. Nielsen,J.S., Lei,L.K., Ebersbach,T., Olsen,A.S., Klitgaard,J.K., Valentin-Hansen,P. and Kallipolitis,B.H. (2010) Defining a role for Hfq in Gram-positive bacteria: evidence for Hfq-dependent antisense regulation in *Listeria monocytogenes*. *Nucleic Acids Res.*, **38**, 907–919.
61. Heidrich,N., Moll,I. and Brantl,S. (2007) In vitro analysis of the interaction between the small RNA SR1 and its primary target ahrC mRNA. *Nucleic Acids Res.*, **35**, 4331–4346.
62. Gaballa,A., Antelmann,H., Aguilar,C., Khakh,S.K., Song,K.B., Smaldone,G.T. and Helmann,J.D. (2008) The *Bacillus subtilis* iron-sparing response is mediated by a Fur-regulated small RNA and three small, basic proteins. *Proc. Natl Acad. Sci. USA*, **105**, 11927–11932.
63. Felden,B., Vandenesch,F., Bouloc,P. and Romby,P. (2011) The *Staphylococcus aureus* RNome and its commitment to virulence. *PLoS Pathog.*, **7**, e1002006.
64. Bohn,C., Rigoulay,C. and Bouloc,P. (2007) No detectable effect of RNA-binding protein Hfq absence in *Staphylococcus aureus*. *BMC Microbiol.*, **7**, 10.
65. Rochat,T., Bouloc,P., Yang,Q., Bossi,L. and Figueroa-Bossi,N. (2012) Lack of interchangeability of Hfq-like proteins. *Biochimie*, **94**, 1554–1559.
66. Wilusz,C.J. and Wilusz,J. (2013) Lsm proteins and Hfq: Life at the 3′ end. *RNA Biol.*, **10**, 592–601.
67. Bandyra,K.J., Said,N., Pfeiffer,V., Gorna,M.W., Vogel,J. and Luisi,B.F. (2012) The seed region of a small RNA drives the controlled destruction of the target mRNA by the endoribonuclease RNase E. *Mol. Cell*, **47**, 943–953.